Energy Minimization of Single-Walled Titanium Oxide Nanotubes

Judy N. Hart,[†,§] Stephen C. Parker,[‡,*] and Alexei A. Lapkin[†]

[†]Department of Chemical Engineering and [‡]Department of Chemistry, University of Bath, Bath BA2 7AY, United Kingdom. [§]Current address: School of Chemistry, University of Bristol, Bristol BS8 1TS, United Kingdom

ABSTRACT Different crystal structures have been proposed as a basis for titanium oxide nanotubes. We have used atomistic simulation techniques to calculate the relative stability of nanotubes with these different crystal structures. Our approach is to use energy minimization, where the total interaction energy is calculated with interatomic potentials based on the Born model of solids. The results reveal nanotubes with the trititanate structure to be the most stable (at unit activity for water). Indeed, nanotubes with the trititanate structure were found to be thermodynamically more favorable than bulk trititanate for nanotube diameters greater than ~8 nm. However, the formation of cross-linking bonds between layers of the trititanate structure occurred frequently; this problem was eliminated by replacing two out of three Ti^{4+} ions with Ti^{3+} ions, although this resulted in a higher energy. Of the structures that do not contain hydrogen, chiral nanotubes made from (101) sheets of anatase are the lowest in energy, suggesting that this is the most likely structure for nanotubes synthesized at low water chemical potential. In general, the stability of the nanotubes increased as the nanotube diameter increased.

KEYWORDS: energy minimization · titanium oxide · nanotubes · trititanate

Titanium oxide nanotubes have attracted much interest in recent years for a range of applications, including hydrogen storage,[1,2] photocatalysts,[3] and dye-sensitized solar cells.[4] The nanotubes are usually synthesized by a hydrothermal reaction.[1,5,6] They typically have an external diameter of ~8−10 nm,[5−7] a length of between ~100 nm and ~10 μm,[1,5,6] and consist of between approximately three and five layers.[6,7] The internal diameter is typically ~5 nm, and the interlayer spacing is ~0.7−0.9 nm.[7,8] It has been suggested that the nanotubes have some degree of chirality (*i.e.*, the angle between the tube axis and the chain of TiO_6 octahedra is not 90°).[1]

The crystal structure of titanium oxide nanotubes remains unclear, and this is hampering efforts to explain the formation mechanism of the nanotubes.[9] Several structures have been proposed, including trititanate ($H_2Ti_3O_7$),[10] a lepidocrocite-like structure ($H_xTi_{2-x/4}\square_{x/4}O_4$ where $x \sim 0.7$ and □ is a vacancy),[7] and anatase.[11,12]

The structure of the nanotubes is difficult to ascertain unambiguously from experimental results.[13] Therefore, in this work, the static energy minimization technique METADISE[14] (minimum energy techniques applied to dislocation, interface, and surface energies) is used to investigate the relative stability of these structures both in bulk form and in the form of nanotubes. The effect of the valence state of titanium on the relative stability of the nanotubes is also investigated.

RESULTS AND DISCUSSION

Bulk Energies. The calculated unit cell parameters for the structures investigated in this work are shown in Table 1. The error in the calculated values is less than 3%. The lattice energies of the bulk structures for lepidocrocite, trititanate, and anatase are shown in Table 2.

TABLE 1. Experimental and Calculated Lattice Parameters for Titanium Oxide Crystal Structures

	experimental	calculated	error (%)
trititanate (monoclinic)			
a/Å	16.03[a]	16.122	0.6
b/Å	3.75[a]	3.690	1.6
c/Å	9.19[a]	9.451	2.8
β	101.45[a]	101.661	1.8
lepidocrocite (orthorhombic, all titanium ions Ti^{3+})			
a/Å	3.783[b]	3.828	1.2
b/Å	18.735[b]	18.843	0.6
c/Å	2.978[b]	3.069	3.1
anatase (tetragonal)			
a,*b*/Å	3.785[c]	3.748	1.0
c/Å	9.514[c]	9.759	2.6

[a]From ref 15. [b]From ref 7. [c]From ref 16.

The anatase structure was found to have the lowest lattice energy, as would be expected. Lepidocrocite has the highest

*Address correspondence to s.c.parker@bath.ac.uk.

Received for review July 2, 2009 and accepted October 13, 2009.

Published online October 21, 2009.
10.1021/nn900723f CCC: $40.75

TABLE 2. Lattice Energies for Various Crystal Structures of Titanium Oxide[a]

structure	atomic formula	valence state of titanium ions	lattice energy per Ti (kJ mol^{-1})
trititanate	$H_2Ti_3O_7$	4+	−11932
lepidocrocite	TiO_2	4+	−11876
lepidocrocite	HTi_2O_4	1:1 mixture of 4+ and 3+	−11822
lepidocrocite	$HTiO_2$	3+	−11768
anatase	TiO_2	4+	−11944

[a]Note that the lattice energy values have been corrected to account for the different compositions, as discussed in the text.

energy, while the lattice energy of trititanate is only marginally higher than that of anatase. Changing the valence state of the titanium ions from 4+ to 3+ in lepidocrocite increases the lattice energy. (Note that the energy of trititanate has been adjusted to account for the fact that it contains hydrogen, while anatase and lepidocrocite contain only titanium and oxygen when all of the titanium ions are Ti^{4+}. The correction was calculated by first using an *ab initio* method[17−20] to determine the expected change in energy for the reaction $TiO_2(s) + 2H_2O(g) \rightarrow Ti(OH)_4(g)$. This value was then used to calculate the energy change associated with adding 1 mol of gaseous water with unit activity to TiO_2 in the energy minimization calculations. Similarly, a correction for the different valence states of titanium was also applied. A more comprehensive description of the method for applying these corrections is given in the Supporting Information.)

For the lepidocrocite structure, there are different possibilities for the position of the layers relative to each other (Figure 1). The structure shown in Figure 1a was found to have the lowest energy when the titanium ions were either all Ti^{4+} or Ti^{3+}. Interestingly, when the titanium ions were a mixture of Ti^{4+} and Ti^{3+} and the initial position of the layers relative to each other was as shown in Figure 1a, it was found that the layers rearranged during energy minimization to the structure shown in Figure 1b, in which the hydrogen bonding interactions between adjacent layers of the structure are shorter; the relative position of the layers in this structure corresponds to that of the lepidocrocite structure proposed by Ma *et al.*[7]

Surface Energies. In attempting to calculate the surface energies for trititanate, it was found that cross-linking occurred between the layers at the cut surface as it was relaxed (Figure 2). This suggests that adjacent surfaces of trititanate are unstable and there is a tendency for a phase transformation to occur, either to a new crystal structure or to an amorphous phase; a possible explanation of this instability is discussed below. Therefore, it was only possible to calculate surface energies for the (001) and (100) surfaces (Table 3). The (100) surface has very low energy, as expected, because there is only van der Waals and hydrogen bonding interactions between layers of this surface (Figure 3a).

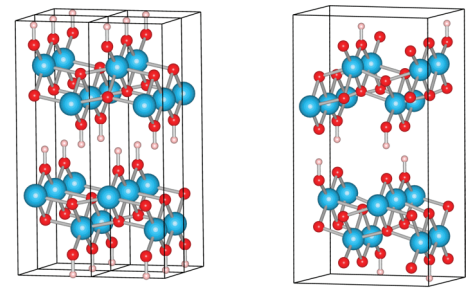

(a) (b)

Figure 1. Two different possibilities for the arrangement of the layers in lepidocrocite relative to each other: (a) lowest energy layer stacking when all titanium ions have the same valence state; (b) lowest energy layer stacking when the titanium ions are a 1:1 mixture of Ti^{4+} and Ti^{3+} (large blue circles, titanium; red circles, oxygen; small white circles, hydrogen).

It was found that, if two out of three of the Ti^{4+} ions were replaced with Ti^{3+} ions, with additional H^+ for charge compensation, this cross-linking at the surfaces no longer occurred and it was possible to calculate the surface energies (Table 4). The composition in this case is $H_4Ti_3O_7$, where 2/3 of the titanium ions are Ti^{3+} and the remainder are Ti^{4+}. The H^+ atoms added for charge compensation are bonded to the undercoordinated oxygen at the edges of the layers (Figure 3b).

For the two surfaces for which values are available for comparison, the surface energy was found to decrease when some of the titanium ions were changed from Ti^{4+} to Ti^{3+}. This is consistent with a reduction in the extent of hydrogen bonding across the surfaces due to the absence of unsaturated O^{2-} with the addition of H^+ for charge compensation. In particular, the surface energy of the (100) surface was very low because interaction between layers of this surface is now dominated by weak van der Waals interactions.

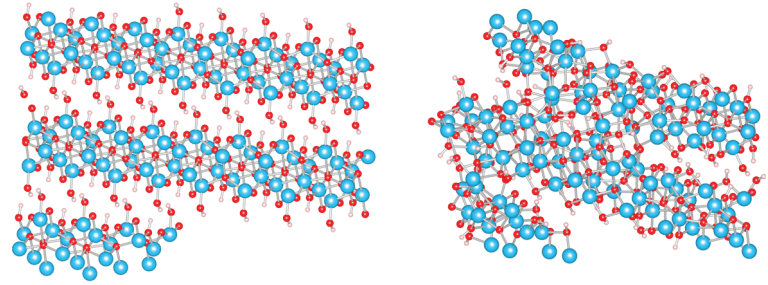

(a) (b)

Figure 2. Cross-linking between layers of the trititanate structure during relaxation of the (011) surface: (a) before relaxation (the cut surface is at the left-hand edge of the image); (b) after relaxation (large blue circles, titanium; red circles, oxygen; small white circles, hydrogen).

TABLE 3. Surface Energies for Trititanate

surface	energy (J m^{-2})
001	1.59
100	0.22

These changes in the interactions between adjacent layers in the trititanate structure are also consistent with the difference in the lattice energies. The lattice energy of the structure with some Ti^{4+} ions changed to Ti^{3+} was −11 827 kJ/mol, significantly higher than when all of the titanium ions were Ti^{4+}. In the structure with only Ti^{4+}, favorable hydrogen bonding interactions occur between hydrogen and oxygen ions in adjacent layers (Figure 3a), while for the structure with Ti^{3+}, the surface of each layer is saturated with hydrogen and weak van der Waals interactions between layers are dominant (Figure 3b). An alternative stacking of the layers for the structure with Ti^{3+} gives a slightly lower lattice energy of −11 832 kJ/mol, consistent with the shorter distances between hydrogen and oxygen (in OH groups) in adjacent layers (Figure 3c).

The formation of cross-linking at cut surfaces of trititanate with only Ti^{4+} may be related to the disruption of the hydrogen bonds that form between layers in the bulk material. The disruption of these bonds leads to reconstruction and cross-linking at the surface. When some Ti^{4+} ions are replaced with Ti^{3+} and the surface of each layer is saturated with protons, interactions between adjacent layers are weaker, so the driving force to form new bonds when the interlayer interactions are disrupted is less significant.

With this change in the oxidation state of the titanium ions, the lattice parameters of trititanate were found to change (Table 5). The change in the *b* and *c* lattice parameters was negligible. There was a significant change in the α and β lattice parameters; this is to be expected because these lattice parameters depend on the interactions between the layers, which change with the change in the titanium oxidation state due to the protons that are added for charge compensation.

The surface energies of the low index surfaces of lepidocrocite are shown in Table 6. The surface energy for the (010) surface is lower than for the other surfaces because, as for the (100) surface of trititanate, there are only van der Waals interactions (and, when Ti^{3+} ions are present, also hydrogen bonding interactions) between layers of this surface.

TABLE 4. Surface Energies for Trititanate with Two out of Three Ti^{4+} Ions Replaced with Ti^{3+} and Additional H^+ for Charge Compensation

surface	energy (J m^{-2})
001	0.66
100	0.02
010	0.35

TABLE 5. Calculated Lattice Parameters for Trititanate (Monoclinic) with Two out of Three Ti^{4+} Ions Replaced with Ti^{3+}

cell parameter	calculated value
a/Å	17.67
b/Å	3.70
c/Å	9.40
β	102.50

The surface energies for the structure containing a 1:1 mixture of Ti^{4+} and Ti^{3+} ions are usually lower than for the structures with all of the titanium ions in the same oxidation state. This may be related to the ability of the structure with a mixture of titanium oxidation states for hydrogen bonding interactions to form between the hydrogen atoms and undercoordinated oxygen atoms by reconstruction of the cut surfaces. (This is only possible in the structure with a mixture of titanium oxidation states because, in this state, undercoordinated oxygen ions are present that can interact with neighboring hydrogen atoms. When all of the titanium ions are Ti^{4+}, there is no hydrogen present, while when all of the titanium ions are Ti^{3+}, the structure is saturated with hydrogen and there is no undercoordinated oxygen.) The exception to this is the (010) surface, which has a higher energy when a mixture of titanium oxidation states is present due to the presence of relatively extensive hydrogen bonding interactions between (010) layers that are broken at the cut surface. Reconstruction of the cut (010) surface to allow new hydrogen bonding interactions to form between atoms at the surface does not occur, resulting in a relatively high surface energy. The surface energies for the structure in which all of the titanium ions are Ti^{4+} tend to be the highest (again with the exception of the (010) surface, due to the absence of hydrogen bonding between these surfaces).

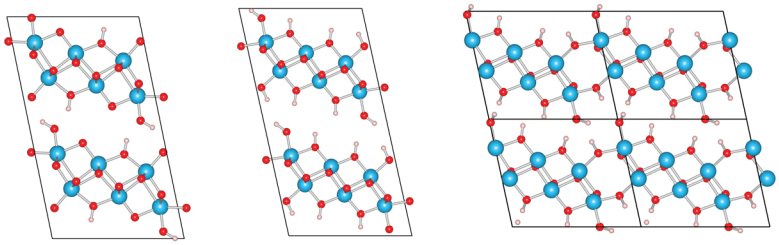

Figure 3. Optimized structures of bulk trititanate, with (a) only Ti^{4+}, (b) two out of three Ti^{4+} replaced with Ti^{3+} and additional H^+ for charge compensation, and (c) same composition as (b) but alternative stacking of the layers (large blue circles, titanium; red circles, oxygen; small white circles, hydrogen).

For anatase, the calculated surface energies were found to be the same as those reported previously (to within 0.01 J/m^2).[21]

TABLE 6. Surface Energies for Lepidocrocite

	energy (J m^{-2})		
surface	all Ti^{4+} ions	1:1 mix of Ti^{4+} and Ti^{3+} ions	all Ti^{3+} ions
001	1.36	1.18	1.30
010	0.04	0.15	0.11
100	3.47	1.32	2.60
011	1.31	1.01	1.22
101	2.89	0.66	2.16
110	2.28	0.27	2.49
111	2.75	1.37	2.07

Nanotube Energies. ***Trititanate.*** Nanotubes were made with (100) sheets of trititanate because this is the surface that was found to have the lowest energy (Table 3) and this is the structure that has been proposed for titanium oxide nanotubes.[10] Energy as a function of nanotube diameter is shown in Figure 4 for both chiral and symmetrical nanotubes. The number of data points in Figure 4 is limited because the nanotube geometry is only stable for a narrow range of diameters (possible reasons for this are discussed below). Over the range of diameters for which the nanotube geometry is stable, the energy generally decreases as the nanotube diameter increases. It can be seen in the optimized structures that hydrogen bonds appear to form between hydrogen and oxygen at the surfaces of the nanotubes (Figure 5a). Thus, the hydrogen bonding interactions that occur between adjacent layers in the bulk material are also able to occur between atoms at the curved surfaces of the nanotubes; this reduces the surface energy of the nanotubes and thus counters the energy increase associated with the dramatic increase in surface area accompanying nanotube formation, resulting in nanotubes that are low in energy. The formation of hydrogen bonds at the curved nanotube surfaces also counterbalances the strain induced by nanotube formation. For symmetrical nanotubes with a diameter of ~6 nm, the length of these hydrogen bonds is ~2.00 nm at the inner surface and ~2.26 nm at the outer surface of the nanotube (compared with hydrogen bond distances of ~1.75 and ~1.93 nm between adjacent layers of bulk trititanate). As the nanotube diameter increases, the hydrogen bonds become significantly shorter at the outer surface (~2.17 nm for a nanotube diameter of ~12 nm), which, in addition to the reduced strain energy for larger nanotube diameters, is consistent with the lower energy of these nanotubes. In fact, for nanotube diameters ≳8 nm, the energy of the nanotubes is less than that of bulk trititanate, indicating that the nanotubes are thermodynamically more favorable than the bulk phase.

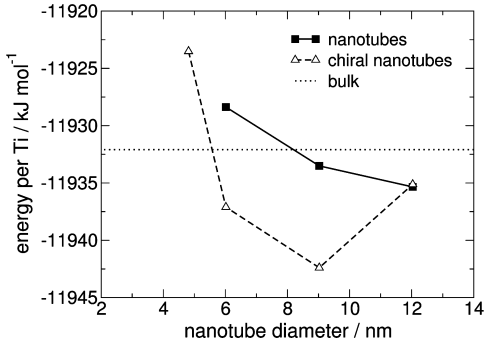

Figure 4. Energy as a function of diameter for nanotubes made from (100) sheets of trititanate; all titanium ions are Ti^{4+}.

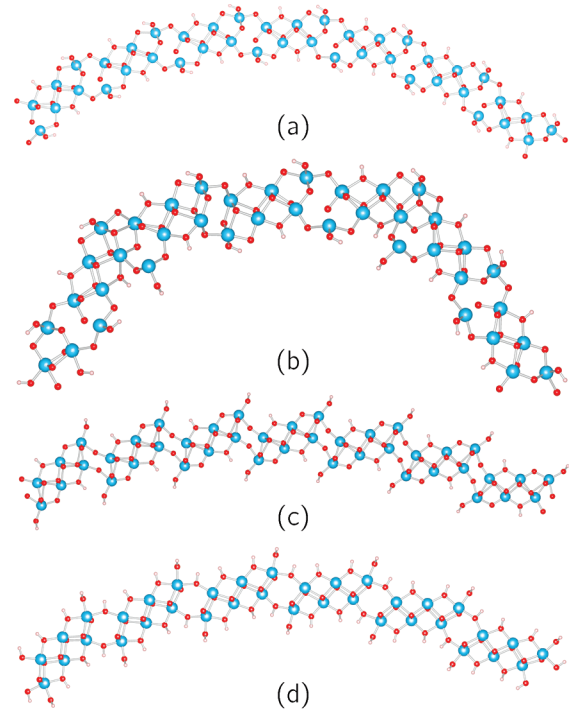

Figure 5. Cross section of trititanate nanotubes after energy minimization: (a) diameter of ~9 nm; (b) diameter of ~4.8 nm; (c) diameter of ~15 nm; (d) diameter of ~9 nm, with two out of three Ti^{4+} ions replaced with Ti^{3+} (large blue circles, titanium; red circles, oxygen; small white circles, hydrogen).

In the case of chiral nanotubes, for a diameter of ~12 nm, the hydrogen bond distances are very similar to those for symmetrical nanotubes and the energies are also very close (Figure 4). Chiral nanotubes with diameters of ~6 and ~9 nm have particularly short hydrogen−oxygen distances at the nanotube surfaces (≲2.08 nm), consistent with the relatively low energy of these nanotubes (Figure 4).

The trititanate nanotubes (both chiral and symmetrical) are only stable for a narrow range of diameters (~5−12 nm). For diameters ≲5 nm, the nanotube geometry was not stable for symmetrical nanotubes because the atomic structure of the nanotubes becomes increasingly distorted as the diameter decreases (Figure 5b). For chiral nanotubes, the nanotube geometry was still stable at a diameter of ~4.8 nm, but the energy was high, consistent with the increase in strain and distortion associated with forming nanotubes as the diameter decreases (seen, for example, by a decrease in the oxygen−oxygen separation at the inner surface of the

TABLE 7. Decrease in Diameter and Wall Thickness for Trititanate Symmetrical Nanotubes Relative to the Expected Values Based on Optimized Bulk Lattice Parameters

nanotube diameter (nm)	decrease in nanotube diameter (%)	decrease in nanotube wall thickness (%)
6.0	12.7	17.6
9.0	8.3	19.3
12.0	6.5	19.9

nanotubes). Similarly, the nanotube geometry was not stable for diameters ≳12 nm (both symmetrical and chiral nanotubes); it can be seen that close hydrogen bonding interactions do not occur for nanotubes with these relatively large diameters (hydrogen−oxygen separations are at least 2.5 nm for nanotubes with a diameter of ~15 nm, Figure 5c), suggesting that the curvature of the surface is important for the formation of these bonds. The range of diameters over which the nanotubes are stable is consistent with diameters of ~8−10 nm reported for synthesized nanotubes.[5−7]

A small positive surface energy was calculated (~0.06 J/m^2) for nanotubes with a diameter of ~6.0 nm. (The nanotube surface energies were calculated by first calculating the energy of an equivalent unrolled slab. The difference between the energy of the nanotube and the unrolled slab was taken to be the difference between the energy of a flat surface (the values for which are presented in the previous section) and the nanotube surface energy. Thus, the energy difference between the slab and the nanotube was divided by the total surface area of the nanotube (including both inner and outer surfaces and taking into account changes in the diameter that occur during energy minimization), and this value was the added to the previously calculated energy of the flat surface.) Interestingly, for larger diameters (≳8 nm), the calculations predict that the surface energy of the nanotubes is negative; that is, the energy of the nanotubes is lower than the bulk energy. These results support the conclusion from the total energy values that these nanotubes are thermodynamically more favorable than bulk trititanate. This concept that, for certain materials, the nanostructure is the most stable morphology is not new.[22]

The diameter of the trititanate nanotubes after energy minimization is smaller than would be expected based on the lattice cell dimensions, with the magnitude of this reduction decreasing as the nanotube diameter increases (Table 7). Similarly, the thickness of the nanotube wall is significantly reduced, with this effect increasing as the nanotube diameter increases. This suggests that a contraction of the structure occurs during the minimization, consistent with the formation of hydrogen bonds at the surfaces of the nanotube, which pull the surface groups inward. The reduction in the

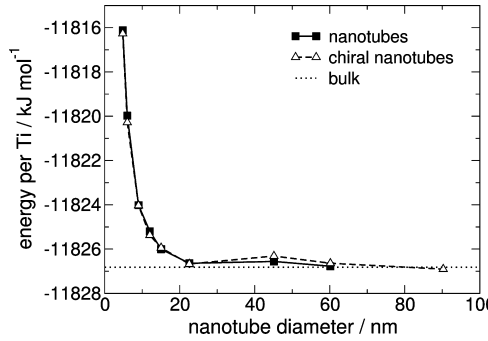

Figure 6. Energy as a function of diameter for nanotubes made from (100) sheets of trititanate, with two out of three Ti^{4+} ions replaced with Ti^{3+} and additional H^+ for charge compensation.

nanotube diameter and wall thickness may also reduce the strain associated with nanotube formation (for example, the Ti−Ti separation in the nanotubes with a diameter of ~6 nm is much closer to that in bulk trititanate after minimization than before).

As seen in Figure 4, in many cases, the trititanate nanotubes are not stable. Therefore, two out of three Ti^{4+} ions were replaced with Ti^{3+}, as was done to calculate the energies of the unstable trititanate surfaces. The energy as a function of nanotube diameter with this change in the oxidation state of the titanium ions is shown in Figure 6.

With two out of three Ti^{4+} ions replaced with Ti^{3+}, all of the nanotube geometries tested are stable. As seen previously, the energy decreases as the nanotube diameter increases. The energy of the chiral nanotubes is very similar to that of the symmetrical nanotubes. For diameters ≳20 nm, the nanotube energy is very close to the bulk energy, although, in contrast to the trititanate nanotubes in which all titanium ions are Ti^{4+}, the nanotube energy is never significantly less than the bulk energy.

In contrast to the results obtained when all titanium ions are Ti^{4+}, with some Ti^{3+} in the structure, the surface energies are positive for all nanotube diameters, although they reach approximately zero for diameters ≳20 nm, suggesting that the bulk material and nanotubes have approximately the same energy for these diameters.

The energy of the nanotubes with a significant Ti^{3+} content is higher than for the nanotubes with only Ti^{4+}, consistent with the higher energy of the bulk material. In the case of the nanotubes with Ti^{3+}, the nanotube surface is saturated with hydrogen, so there are no possible sites for hydrogen bonding interactions at the nanotube surface (Figure 5d). Thus, a possible explanation of the relatively high energy of nanotubes containing Ti^{3+} is that favorable interactions between groups at the surface of the nanotubes are not able to offset the strain energy associated with nanotube formation, and the energy of the nanotubes is therefore higher than that of the bulk material.

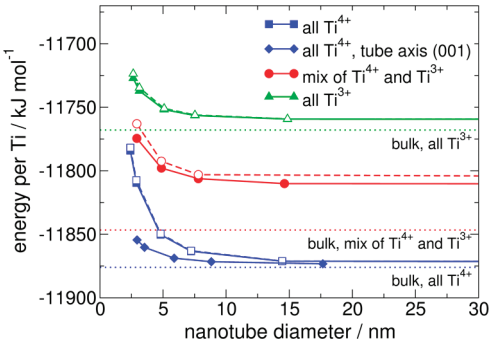

Figure 7. Energy as a function of diameter for nanotubes made from (010) sheets of lepidocrocite. The tube axis is parallel to the (100) direction of the lepidocrocite structure, except where stated otherwise. Filled symbols and solid lines, symmetrical nanotubes; open symbols and dashed lines, chiral nanotubes.

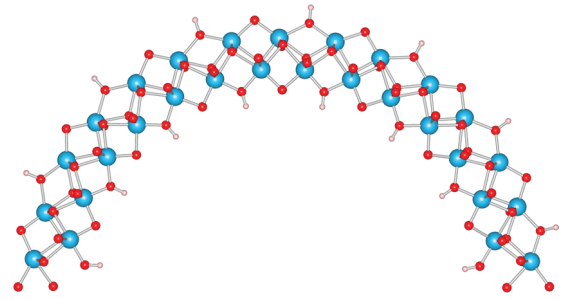

Figure 8. Section of a lepidocrocite nanotube (in which half of the titanium ions are Ti^{4+} and half are Ti^{3+}) after energy minimization; in contrast to the behavior of trititanate, hydrogen bonding interactions do not form between hydrogen and undercoordinated oxygen ions at the nanotube surface (large blue circles, titanium; red circles, oxygen; small white circles, hydrogen).

These results for the effect of the titanium oxidation state on the energy of the nanotubes indicate that the titanium ions are most likely to be Ti^{4+}. This is consistent with experimental results, which show that the nanotubes are white, not black, as they would be expected to be with if there were a significant Ti^{3+} content. However, these results for nanotubes with Ti^{3+} suggest that surface groups strongly influence the structure and stability of the nanotubes. It has been seen that neighboring surfaces of trititanate, $H_2Ti_3O_7$, are unstable and form cross-links across surfaces, but increasing the concentration of surface hydrogen stabilizes the surfaces.

The energy of a double-layered nanotube was calculated for trititanate containing Ti^{3+}, consisting of nanotubes with diameters of 4.8 and 6.0 nm. The energy was found to be −11 819.3 kJ/mol, slightly lower than the combined energy of the two single-layered nanotubes (−11 818.5 kJ/mol), thus supporting the experimental observation that titanium oxide nanotubes are multilayered. It was not possible to determine the energy of a double-layered nanotube in the case of all the titanium ions being Ti^{4+}, due to cross-linking occurring between the layers of the nanotube.

Lepidocrocite. Nanotubes were made from (010) sheets of lepidocrocite because this surface was found to have the lowest energy (Table 6), and this is the structure that has been proposed for titanium oxide nanotubes.[7] Nanotubes with both the (100) and the (001) directions parallel to the nanotube axis were investigated. The energy as a function of the nanotube diameter for both chiral and symmetrical nanotubes, for the different oxidation states of the titanium ions, is shown in Figure 7.

In all cases, the energy of the nanotubes decreases as a function of the nanotube diameter, and the energy of the chiral nanotubes is slightly higher than that of the symmetrical nanotubes. When the nanotube axis is parallel to the [100] direction, the magnitude of the change in energy over the range of nanotube diameters investigated is significantly larger when all of the titanium ions are Ti^{4+} rather than Ti^{3+}. This may be related to close interactions between negatively charged oxygen ions around the inner surface of the very small nanotubes; for example, the oxygen separation is only 2.48 Å when all of the titanium ions are Ti^{4+} (for the smallest nanotube diameter), compared with 2.59 Å when all of the titanium ions are Ti^{3+}, which raises the energy of the nanotubes with small diameters. In the case of the titanium ions being a mixture of Ti^{4+} and Ti^{3+}, the nanotube geometry is not stable for diameters less than ~3 nm, indicating that this diameter is the lower limit for stable nanotubes with a 1:1 mixture of Ti^{4+} and Ti^{3+}.

For trititanate, it was seen that hydrogen bonding interactions form at the surface of the nanotubes in place of the interactions that occur between adjacent layers in the bulk material, thus stabilizing the nanotubes. For lepidocrocite, the only oxidation state for which this is might feasibly occur is the mixture of Ti^{4+} and Ti^{3+} (for the same reasons as outlined in the discussion of surface energies above). However, while hydrogen bonds form between adjacent layers in the bulk material, it was found that for lepidocrocite the nanotube geometry is not compatible with the formation of hydrogen bonds at the nanotube surface and the distance between the protons and the oxygen ions was always greater than 2.5 Å after relaxation (Figure 8). It is possible that, at smaller diameters, these separations cannot be maintained and interactions between groups at the nanotube surface (particularly the inner surface) cause distortion of the nanotube geometry, which may partly explain the observed instability of the nanotubes with diameters <3 nm.

When the nanotube axis is parallel to the [001] direction and all of the titanium ions are Ti^{4+}, the oxygen−oxygen separation at the inner surface of the nanotube is significantly larger (3.15 Å for the smallest nanotube diameter) than when the nanotube axis is parallel to the [100] direction, and the energy of the nanotubes is correspondingly lower, in agreement with

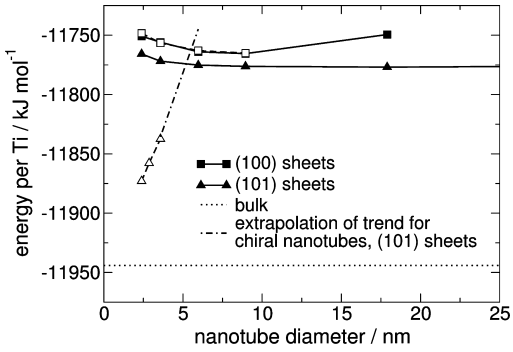

Figure 9. Energy as a function of diameter for nanotubes made from (101) and (100) sheets of anatase; the valence state of the titanium ions is 4+. Filled symbols and solid lines, symmetrical nanotubes; open symbols and dashed lines, chiral nanotubes.

the results of Enyashin and Seifert.[23] However, for large nanotubes (diameter $\gtrsim$20 nm), there is no significant difference in the energies of the nanotubes with the [001] and [100] directions parallel to the tube axis.

In contrast to the result for trititanate, all surface energy values are positive for lepidocrocite. As an indicative value, the surface energy of the nanotubes with large diameters is $\sim$0.08 J/m^2 when all of the titanium ions are Ti^{4+}.

For large nanotube diameters, the magnitude of the difference between the nanotube energy and the energy of the bulk material corresponds to the calculated surface energy for the (010) surface of lepidocrocite (*i.e.*, the surface energy was calculated to be the lowest for the case of all of the titanium ions being Ti^{4+} and the highest when the titanium ions were a mixture of Ti^{4+} and Ti^{3+}, and these correspond, respectively, to the smallest and largest differences between the nanotube energy and the lattice energy of lepidocrocite for large nanotube diameters). The reason for this is that, as the nanotube diameter increases toward the limit of infinity, the strain energy associated with wrapping a flat sheet to form a nanotube decreases and the most significant factor causing the energy of the nanotube to be greater than the energy of the bulk material is the increased surface area.

Regardless of the oxidation state of the titanium ions, the inner diameter of the lepidocrocite nanotubes is smaller after energy minimization than would be expected based on the unit cell parameters, as was the case for trititanate; the magnitude of this reduction decreases as the nanotube diameter increases. In addition, the wall thickness of the smallest nanotubes is less than for a flat sheet of lepidocrocite, but again, the magnitude of this reduction decreases as the nanotube diameter increases. This contraction of the structure reduces the strain associated with nanotube formation, particularly in the outer wall of the nanotubes.

For the case of all of the titanium ions being Ti^{4+}, the energy of a double-layered nanotube was calculated. The inner diameter of this double-layered nanotube was $\sim$2.9 nm, and the interlayer spacing was $\sim$0.8 nm, within the range of the interlayer spacing found in experimental work ($\sim$0.7$-$0.9 nm).[7,8] The energy of this double-layered nanotube was found to be $-$11 831.5 kJ/mol, slightly lower than the combined energy of the two single-layered nanotubes ($-$11 830.6 kJ/mol), as was the case for the double-layered nanotube with the trititanate structure.

Anatase. Nanotubes made with both (101) and (100) sheets of anatase were investigated because the surface energies are similar. The energy of the nanotubes made from (101) sheets of anatase decreases as the nanotube diameter increases but appears to reach a plateau well above the bulk energy (Figure 9). This relatively high energy compared with the bulk is consistent with the fact that the titanium ions are only five-coordinated in the nanotubes, whereas they are six-coordinated in bulk anatase (Figure 10).

The energy was lower for chiral nanotubes than symmetrical nanotubes of the same diameter, and the energy of the chiral nanotubes increased as the diameter increased (*i.e.*, stability decreased with increasing diameter). This is very different behavior from that seen for other structures. The titanium ions are six-coordinated in the chiral nanotubes after energy minimization (Figure 11), consistent with the lower energy

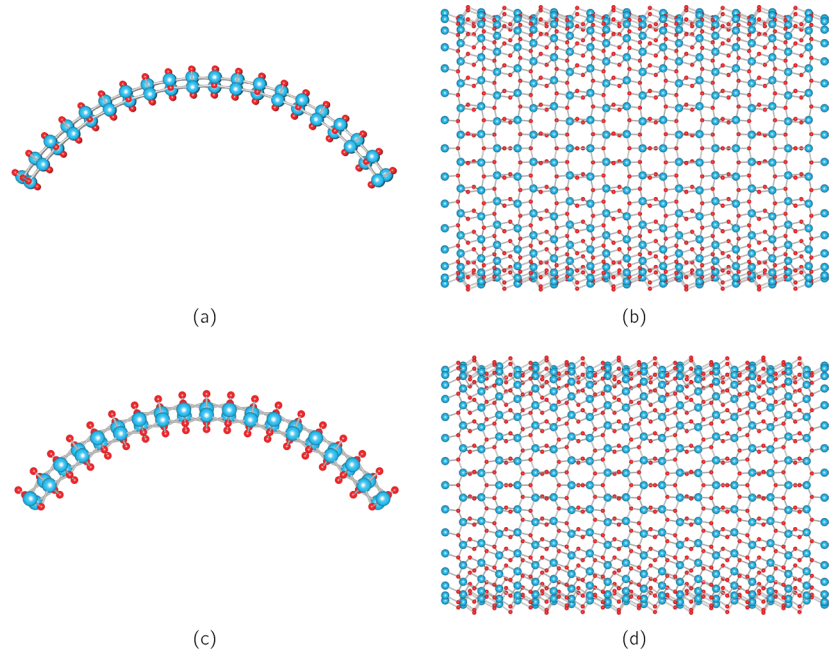

Figure 10. Nanotubes made from (101) sheets of anatase: (a) cross section and (b) nanotube wall before energy minimization; (c) cross section and (d) nanotube wall after energy minimization.

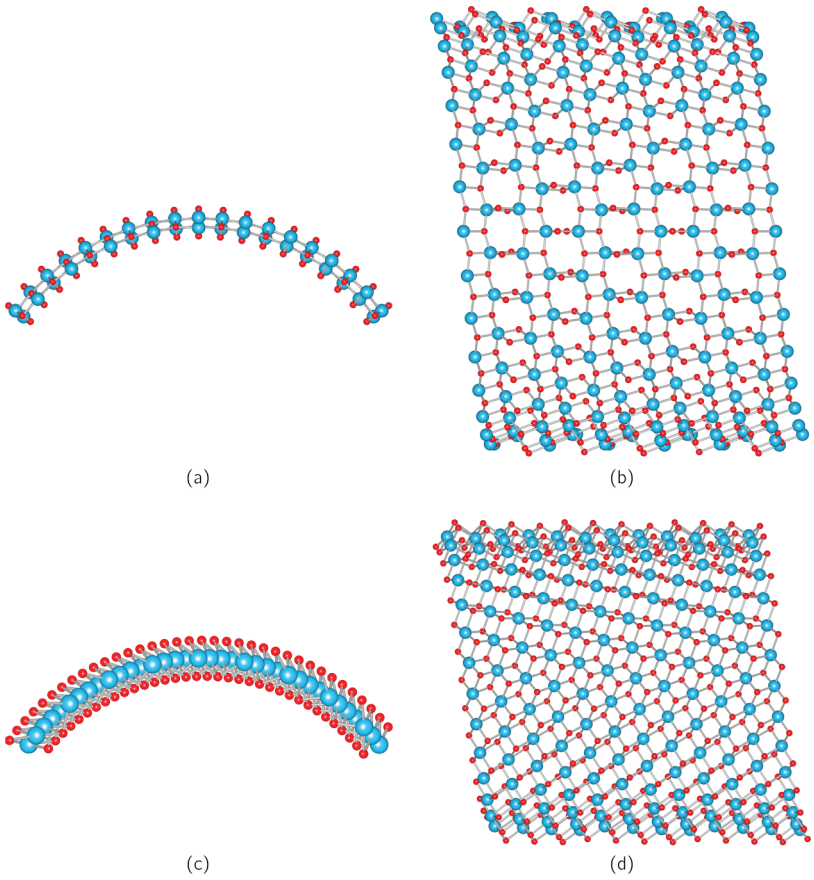

Figure 11. Chiral nanotubes made from (101) sheets of anatase: (a) cross section and (b) nanotube wall before energy minimization; (c) cross section and (d) nanotube wall after energy minimization.

of the chiral relative to the symmetrical nanotubes. The Ti−Ti separations are also larger in the chiral than the symmetrical nanotubes (*e.g.*, 2.84 Å for a chiral nanotube with a diameter of 2.4 nm, compared with 2.74 Å for a symmetrical nanotube with the same diameter; the Ti−Ti separation in bulk anatase is 3.05 Å).

As the diameter increases for the chiral nanotubes, the Ti−O separation increases and the Ti−Ti separation decreases, consistent with the increase in energy (*i.e.*, the nanotubes become less stable). The Ti−Ti separation decreases from 2.84 to 2.80 Å for chiral nanotubes as the diameter increases from 2.4 to 3.6 nm. For the same diameter change, the longest of the six Ti−O bonds increases from 2.18 to 2.21 Å; in contrast, the longest Ti−O bond in anatase is 2.03 Å. For a nanotube diameter greater than ~4 nm, the chiral nanotubes are unstable (*i.e.*, their energy is significantly higher than that of the symmetrical nanotubes), suggesting that the energy *versus* nanotube diameter trend approximately follows the extrapolation shown in Figure 9. However, due to this instability, it was not possible to calculate a value for the energy of chiral nanotubes with diameters $\gtrsim$4 nm.

The energy as a function of the length of the chiral displacement for nanotubes with a diameter of ~3.6 and ~8.9 nm is shown in Figure 12. These results indicate that, for chiral nanotubes (at least up to a chiral displacement of three times the length of the unit cell dimension), the energy of the nanotubes with the smaller diameter is lower than that for the larger diameter nanotubes, in contrast to the results for nanotubes with other structures (*e.g.*, lepidocrocite and trititanate, for which energy was found to decrease with increasing nanotube diameter). As mentioned above, this energy increase with increasing diameter corresponds to larger Ti−O and smaller Ti−Ti separations in the nanotubes with the larger diameters. The Ti−Ti separation is 2.82 Å for nanotubes with a diameter of 8.9 nm and a chiral displacement of two times the unit cell dimension, compared with 2.88 Å for a nanotube diameter of 3.6 nm and the same chiral displacement. Correspondingly, the average Ti−O bond length is 2.02 Å (with a maximum of 2.16 Å) for nanotubes with a diameter of 8.9 nm and a chiral displacement of two times the unit cell dimension, compared with 1.99 Å (maximum of 2.12 Å) for a nanotube diameter of 3.6 nm and the same chiral displacement.

For a nanotube diameter of ~3.6 nm, a minimum in energy occurs for a chiral displacement of three times the length of the unit cell dimension, while for a nanotube diameter of ~8.9 nm, the energy continues to decrease up to a chiral displacement of five times the length of the unit cell dimension. This decrease in energy as the chiral displacement increases can also be related to the increasing Ti−Ti separation (from 2.82 to 2.88 Å for nanotubes with a diameter of 8.9 nm as the chiral displacement increases from two to five times the length of the unit cell, while it is only 2.70 Å for symmetrical nanotubes with the same diameter). The Ti−O separations also decrease as the chiral displacement increases, with the average and maximum Ti−O bond

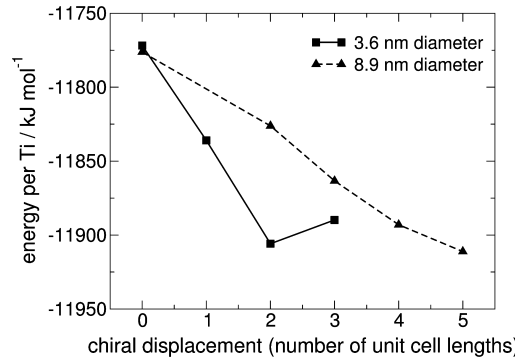

Figure 12. Energy as a function of number of chiral steps for nanotubes (diameter ~3.6 and ~8.9 nm) made from (101) sheets of anatase.

lengths decreasing from 2.02 to 1.99 Å and from 2.16 to 2.10 Å, respectively. The Ti−Ti and Ti−O separations for nanotubes with a diameter of 8.9 nm and a chiral displacement of five times the length of the unit cell are very similar to those for nanotubes with a diameter of 3.6 nm and a chiral displacement of two times the length of the unit cell, and the energies are correspondingly very similar. It is interesting to note that, for a chiral displacement of two or more times the length of the unit cell dimension, the chiral nanotubes become stable even for nanotube diameters as large as ~9 nm (whereas they were only stable up to a diameter of ~4 nm for a chiral displacement of one unit cell).

The energy of nanotubes made from (100) sheets of anatase is higher than that of nanotubes made from (101) sheets, consistent with the higher energy of the (100) surface relative to the (101) surface (2.01 J/m^2 compared with 1.72 J/m^2). As for the symmetrical nanotubes made from (101) anatase sheets, the titanium ions in the nanotubes made from (100) sheets are only five-coordinated, consistent with the high energy of the nanotubes relative to bulk anatase. For nanotubes made from (100) sheets of anatase, there appears to be a minimum in the energy as a function of diameter, occurring at a diameter of ~10 nm (Figure 9). There is very little difference in the energy of the chiral and symmetrical nanotubes (the chiral nanotubes also contain five-coordinated titanium ions), although the energy of the chiral nanotubes is generally slightly higher, consistent with the results for trititanate and lepidocrocite.

The structure of nanotubes made from both (101) and (100) sheets of anatase appears to change significantly during the energy minimization (Figures 10, 11, and 13), and in the case of symmetrical nanotubes made from (100) sheets of anatase, the structure also changes as the nanotube diameter increases (Figure 13). These structural changes during optimization are accompanied by an increase in the minimum O−O separation. For symmetrical nanotubes made from both (101) and (100) sheets of anatase, the O−O separation increases as diameter increases, consistent with the decrease in energy with increasing diameter. The exception to this trend is the nanotubes made from (100) anatase sheets with the largest diameter (17.9 nm), for which the O−O separation decreases, with a corresponding increase in energy, relative to the nanotubes with a smaller diameter of 8.9 nm.

As suggested above, for chiral nanotubes made from (101) sheets of anatase, an even more dramatic structural change occurs during energy minimization, which results in the titanium ions changing from five-coordinated in the original structure to six-coordinated in the relaxed structure (Figure 11). This change in consistent with the relatively low energy of chiral nanotubes made from (101) sheets of anatase.

As for lepidocrocite, all nanotube surface energies were found to be positive. The surface energy of the

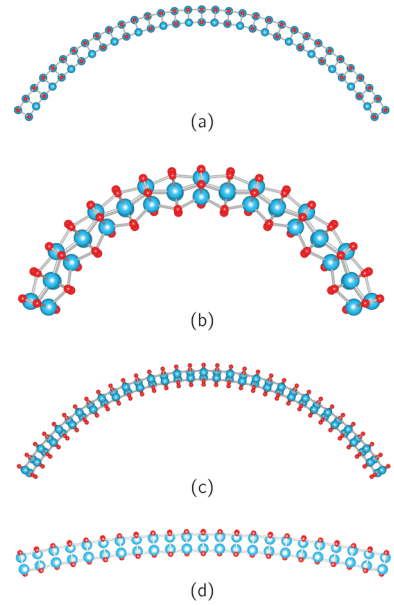

Figure 13. Section of nanotubes made from (100) sheets of anatase (a) with a diameter of 17.9 nm, before energy minimization (the structure was the same for all diameters before minimization), and after minimization with a diameter of (b) 2.4 nm, (c) 6.0 nm, and (d) 17.9 nm.

large diameter nanotubes made from (101) sheets of anatase is ~4.2 J/m^2, significantly higher than the surface energy of a flat sheet of (101) anatase (1.72 J/m^2).

When all of the titanium ions are Ti^{3+} (with charge compensating protons bonded to the undercoordinated oxygen atoms at the internal and external surfaces of the nanotubes), nanotubes made from (100) sheets of anatase are more stable than those made from (101) sheets (Figure 14), in contrast to the case when all of the titanium ions are Ti^{4+}. For all nanotubes in which the titanium ions are all Ti^{3+}, the nanotube geometry is unstable for diameters $\gtrsim$4 nm.

As for the other structures investigated, the diameters of the anatase nanotubes (for nanotubes made from both (101) and (100) sheets of anatase) are smaller than would be expected based on the lattice dimensions. The wall thickness of the nanotubes increased

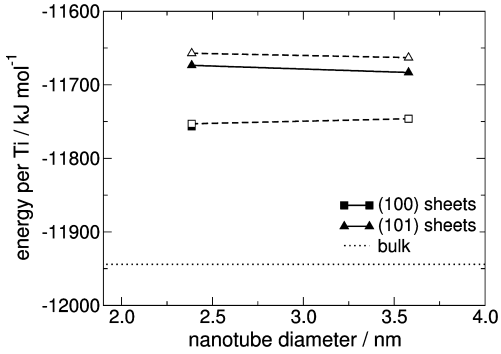

Figure 14. Energy as a function of diameter for nanotubes made from (101) and (100) sheets of anatase; the valence state of the titanium ions is 3+. Filled symbols and solid lines, symmetrical nanotubes; open symbols and dashed lines, chiral nanotubes.

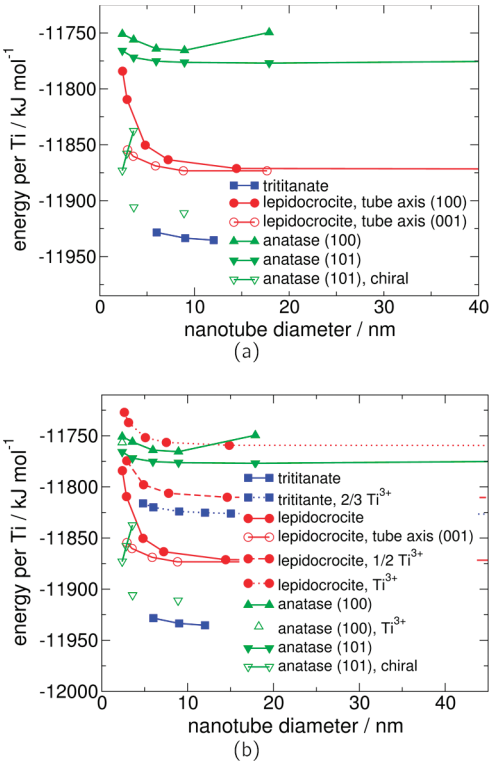

Figure 15. Energy as a function of diameter for nanotubes made from (010) sheets of lepidocrocite (tube axis is parallel to the (100) direction except where stated otherwise), (100) sheets of trititanate, (101) sheets of anatase, and (100) sheets of anatase (for chiral nantoubes made from (101) sheets of anatase, data are included for the three diameters that were stable with one chiral step and also for the number of chiral steps that gave the minimum energy for nanotubes with diameters of 3.6 and 8.9 nm): (a) the oxidation state of all titanium ions is 4+; (b) the oxidation state of the titanium ions is 4+, except where stated otherwise.

significantly during the energy minimization, especially for nanotubes made from (100) sheets of anatase. This can be attributed to the change in the structure that occurs during the energy minimization (Figures 10 and 13).

Comparison of Structures. Across the range of diameters for which the nanotube geometry is stable, the trititanate structure is the lowest in energy (Figure 15); the range of diameters for which the nanotube geometry is stable for trititanate is consistent with the observations for synthesized nanotubes. Symmetrical nanotubes with the anatase structure are the highest in energy (when all of the titanium ions are Ti^{4+}). However, chiral nanotubes with the anatase structure are significantly lower in energy; of the nanotubes containing no hydrogen, the lowest in energy are chiral nanotubes made from (101) sheets of anatase, suggesting that this is the most likely structure for nanotubes synthesized at low water chemical potential. The stability of these anatase nanotubes is very sensitive to both diameter and the extent of chirality. The calculated low energy of chiral nanotubes made from (101) sheets of anatase is consistent with experimental reports that titanate nanotubes are often chiral.[1]

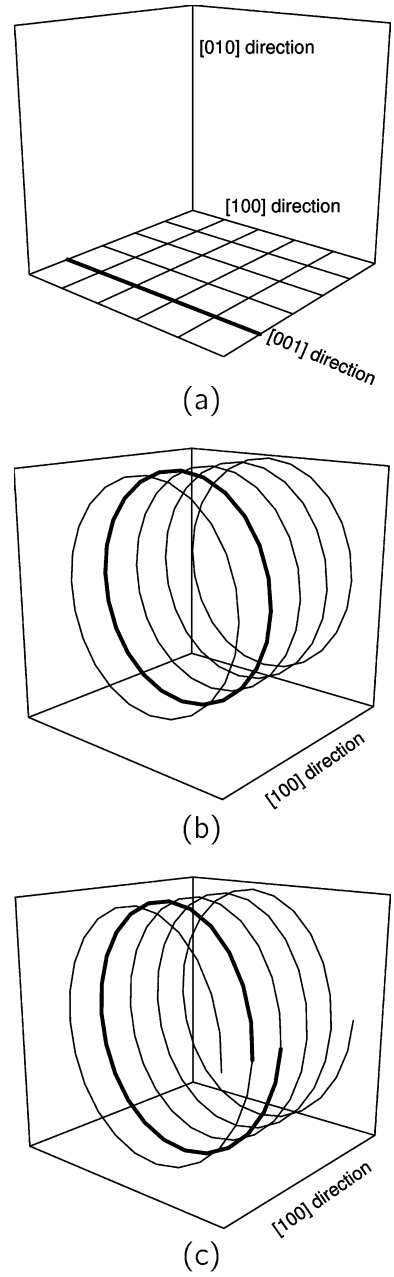

Figure 16. Schematic diagram showing (a) (010) sheet used to make lepidocrocite nanotubes, (b) nanotube made by wrapping the [001] direction to form circles; (c) nanotube made by wrapping the [001] direction to form a helix along the length of the tube; the bold line in each diagram indicates the [001] direction.

For the case when all of the titanium ions are Ti^{3+}, nanotubes made from (100) sheets of anatase are lowest in energy for small nanotube diameters, but for larger nanotube diameters, lepidocrocite is the only structure that produces stable nanotube geometries. The nanotubes containing Ti^{3+} were all higher in energy than those containing only Ti^{4+}, consistent with the experimental observation that the nanotubes are white, rather than black.

The composition of the nanotubes is likely to depend on the chemical potential of water during the

nanotube synthesis. A high water chemical potential is likely to favor nanotubes with a high hydrogen content (*e.g.*, trititanate), while a low water chemical potential will favor structures without hydrogen (*e.g.*, TiO_2, most likely chiral nanotubes made from (101) sheets of anatase rather than lepidocrocite nanotubes). Differences in the water chemical potential during synthesis may partly explain the variety of different structures for the nanotubes that have been reported. Further study of the effects of water chemical potential on the structure of titanate nanotubes, both theoretical and experimental, is required.

Further investigation of multilayered nanotubes is also needed because the results of this study suggest that the nanotube structure predicted to be the lowest in energy for single-layered nanotubes, trititinate, is not stable when it is multilayered, and cross-linking occurs between the layers during energy minimization. This is in contrast to the experimental finding that titanate nanotubes are multilayered. This suggests that multilayer trititante nanotubes may be metastable and may undergo a phase transformation, for example, to form anatase regions, in order to reach a more thermodynamically favorable state. Molecular dynamics simulations at a range of temperatures (beyond the scope of this paper) may help to clarify the stability and phase transformation behavior of multilayered nanotubes. In addition, further simulations that include simulated annealing may be useful future work.

CONCLUSIONS

The most stable structure for titanium oxide nanotubes depends on the activity of water during synthesis. Trititanate was found to be the most stable at unit activity for water, across the range of nanotube diameters investigated. This stability appears to be related to the formation of hydrogen bonding interactions at the nanotube surfaces, and for diameters greater than ~8 nm, trititanate nanotubes are thermodynamically more favorable than bulk trititanate. When hydrogen bonding interactions are not able to occur at the nanotube surfaces, the nanotube geometry is not stable, resulting in the trititanate nanotubes only being stable for a narrow range of diameters. The range of diameters for which these nanotubes are predicted to be stable is in agreement with the observed diameters for synthesized nanotubes. The range of diameters for which the nanotube geometry is stable could be increased by replacing two out of three Ti^{4+} ions with Ti^{3+} ions and including additional protons in the structure to maintain charge neutrality. However, the energy of these nanotubes was greater than that of the trititanate nanotubes with only Ti^{4+} ions.

Of the structures that do not contain hydrogen, nanotubes made by chiral wrapping of (101) sheets of anatase are the lowest in energy, suggesting that this is the most likely structure for nanotubes synthesized at low water chemical potential.

We have not yet investigated all possible compositions that have been proposed, including a structure of lepidocrocite that has been proposed with the formula unit $H_xTi_{2-x/4}\square_{x/4}O_4$ where $x \sim 0.7$ and $\square$ is a vacancy,[7] because the number of atoms required for these simulations would be very large. However, given the low energy of trititanate nanotubes, lepidocrocite is unlikely to exceed it in stability, although the hydrogen content of this lepidocrocite structure is less than that of trititanate, so their relative stability may depend on the water chemical potential during synthesis. Further work must also be undertaken to consider the stability of multilayered nanotubes, as well as the effects of temperature, by molecular dynamics simulations, which of course also allows investigation of the hydrogen storage capabilities of the nanotubes.

METHODS

Energy minimization was performed with the static energy minimization technique METADISE.[14] The Buckingham potential, Φ_{ij} (eq 1), was used for short-range interactions, with the exception of interactions between hydrogen and the oxygen to which they were bonded, which were treated with a Morse potential (eq 2). An oxygen atom attached to a hydrogen atom (denoted by OH) was treated with a different interaction potential from an oxygen atom bonded only to titanium atoms (denoted by O). Electronic polarization of ions was taken into account by representing each ion as a massless shell connected to a core by a harmonic spring. The parameters used in the interatomic potential are shown in Table 1 in the Supporting Information (note that, where applicable, these interaction parameters apply to interactions between shells, rather than cores). We took the potential model parameters from a previous paper describing the potential model and how it had been refined to improve its performance for anatase (the TiO_2 phase of relevance here).[21] The interested reader can return to the original paper for complete details.

$$\Phi_{ij} = A\exp\left(-\frac{r_{ij}}{\rho}\right) - \frac{C}{r_{ij}^6} \quad (1)$$

$$\Phi_{ij} = D[\exp(-2\alpha(r_{ij} - r_0)) - 2\exp(-\alpha(r_{ij} - r_0))] \quad (2)$$

The initial crystal structures were taken from the Chemical Structures Database.[24] The structure for lepidocrocite was taken from the structure for FeO(OH), with Fe(III) replaced with Ti(III).

The bulk structures for lepidocrocite, trititanate, and anatase were relaxed, and the lattice energy was calculated. Similarly, surface energies (for low index surfaces) were calculated after relaxing each surface. Nanotubes were made by wrapping sheets of the titanium oxide, where the exposed surfaces were those with the lowest energy, and then the energy was calculated as a function of the nanotube diameter. The formation of the nanotubes is illustrated in Figure 16 for the case of lepidocrocite; nanotubes were formed by wrapping (010) sheets (Figure 16a) such that the [100] direction was the direction along the axis of the tube, and the [001] direction was wrapped and joined at the edges of the sheet to form either circles (Figure 16b) or a helix along the length of the tube (Figure 16c), thus introducing chirality into the nanotubes. Lepidocrocite nanotubes were also formed by wrapping the (010) sheets in the alternate direction, such that the [001] direction was the direction along the axis of the tube. Similarly, for trititanate, nanotubes

were made from (100) sheets, such that the [010] direction was parallel to the nanotube axis. For anatase, nanotubes were made from both (101) sheets and (100) sheets, such that the tube axis was parallel to the [$\bar{1}$01] and [001] directions, respectively. The chiral displacement was equal to the length of one unit cell dimension in the relevant direction (ranging from ~4 Å for lepidocrocite and trititanate to ~10 Å for anatase).

For simplicity, the formula for lepidocrocite was taken as $H_2Ti_2O_4$. In this structure, the hydrogen positions can be either completely or only partially filled, and the valence state of the titanium ions will change to compensate; therefore, we have investigated three different states (*i.e.*, all titanium ions in the 4+ valence state and no hydrogen, all titanium ions in the 3+ state with all hydrogen sites filled, and a 1:1 mixture of titanium ions in the 3+ and 4+ states with half of the hydrogen sites filled). This use of different valence states also provides a basis for comparison with trititanate, for which the effect of changing the oxidation state of the titanium ions was also investigated.

Acknowledgment. The authors gratefully acknowledge financial support from the EPSRC (Grant No. EP/D039673). We acknowledge the use of the EPSRC's Chemical Database Service at Daresbury.

Supporting Information Available: Additional experimental data and table. This material is available free of charge *via* the Internet at http://pubs.acs.org.

REFERENCES AND NOTES

1. Bavykin, D. V.; Lapkin, A. A.; Plucinski, P. K.; Friedrich, J. M.; Walsh, F. C. Reversible Storage of Molecular Hydrogen by Sorption into Multilayered TiO_2 Nanotubes. *J. Phys. Chem. B* **2005**, *109*, 19422–19427.
2. Lim, S. H.; Luo, J. Z.; Zhong, Z. Y.; Ji, W.; Lin, J. Y. Room-Temperature Hydrogen Uptake by TiO_2 Nanotubes. *Inorg. Chem.* **2005**, *44*, 4124–4126.
3. Lin, C. H.; Lee, C. H.; Chao, J. H.; Kuo, C. Y.; Cheng, Y. C.; Huang, W. N.; Chang, H. W.; Huang, Y. M.; Shih, M. K. Photocatalytic Generation of H_2 Gas from Neat Ethanol over Pt/TiO_2 Nanotube Catalysts. *Catal. Lett.* **2004**, *98*, 61–66.
4. Adachi, M.; Murata, Y.; Okada, I.; Yoshikawa, S. Formation of Titania Nanotubes and Applications for Dye-Sensitized Solar Cells. *J. Electrochem. Soc.* **2003**, *150*, G488–G493.
5. Kasuga, T.; Hiramatsu, M.; Hoson, A.; Sekino, T.; Niihara, K. Titania Nanotubes Prepared by Chemical Processing. *Adv. Mater.* **1999**, *11*, 1307–1311.
6. Chen, Q.; Zhou, W. Z.; Du, G. H.; Peng, L. M. Trititanate Nanotubes Made *via* a Single Alkali Treatment. *Adv. Mater.* **2002**, *14*, 1208–1211.
7. Ma, R. Z.; Bando, Y.; Sasaki, T. Nanotubes of Lepidocrocite Titanates. *Chem. Phys. Lett.* **2003**, *380*, 577–582.
8. Du, G. H.; Chen, Q.; Che, R. C.; Yuan, Z. Y.; Peng, L. M. Preparation and Structure Analysis of Titanium Oxide Nanotubes. *Appl. Phys. Lett.* **2001**, *79*, 3702–3704.
9. Ou, H.-H.; Lo, S.-L. Review of Titania Nanotubes Synthesized *via* the Hydrothermal Treatment: Fabrication, Modification, and Application. *Sep. Purif. Technol.* **2007**, *58*, 179–191.
10. Chen, Q.; Du, G. H.; Zhang, S.; Peng, L. M. The Structure of Trititanate Nanotubes. *Acta Crystallogr.* **2002**, *B58*, 587–593.
11. Kasuga, T.; Hiramatsu, M.; Hoson, A.; Sekino, T.; Niihara, K. Formation of Titanium Oxide Nanotube. *Langmuir* **1998**, *14*, 3160–3163.
12. Wang, W. Z.; Varghese, O. K.; Paulose, M.; Grimes, C. A.; Wang, Q. L.; Dickey, E. C. A Study on the Growth and Structure of Titania Nanotubes. *J. Mater. Res.* **2004**, *19*, 417–422.
13. Bavykin, D. V.; Friedrich, J. M.; Walsh, F. C. Protonated Titanates and Titanium Dioxide Nanostructured Materials: Synthesis, Properties and Applications. *Adv. Mater.* **2006**, *18*, 2807–2824.
14. Watson, G. W.; Kelsey, E. T.; de Leeuw, N. H.; Harris, D. J.; Parker, S. C. Atomistic Simulation of Dislocations, Surfaces and Interfaces in MgO. *J. Chem. Soc., Faraday Trans.* **1996**, *92*, 433–438.
15. Feist, T. P.; Davies, P. K. The Soft Chemical Synthesis f TiO_2(B) from Layered Titanates. *J. Solid State Chem.* **1992**, *101*, 275–295.
16. Howard, C. J.; Sabine, T. M.; Dickson, F. Structural and Thermal Parameters for Rutile and Anatase. *Acta Crystallogr.* **1991**, *B47*, 462–468.
17. Kresse, G.; Furtmüller, J. Efficiency of *Ab-Initio* Total Energy Calculations for Metals and Semiconductors using a Plane-Wave Basis Set. *Comput. Mater. Sci.* **1996**, *6*, 15–50.
18. Kresse, G.; Furtmüller, J. Efficient Iterative Schemes for *Ab Initio* Total-Energy Calculations Using a Plane-Wave Basis Set. *Phys. Rev. B* **1996**, *54*, 11169–11186.
19. Kresse, G.; Hafner, J. *Ab Initio* Molecular Dynamics for Liquid Metals. *Phys. Rev. B* **1993**, *47*, 558–561.
20. Kresse, G.; Hafner, J. *Ab Initio* Molecular-Dynamics Simulation of the Liquid−Metal−Amorphous-Semiconductor Transition in Germanium. *Phys. Rev. B* **1994**, *49*, 14251–14269.
21. Olson, C. L.; Nelson, J.; Islam, M. S. Defect Chemistry, Surface Structures, and Lithium Insertion in Anatase TiO_2. *J. Phys. Chem. B* **2006**, *110*, 9995–10001.
22. Lin, Z.; Gilbert, B.; Liu, Q.; Ren, G.; Huang, F. A Thermodynamically Stable Nanophase Material. *J. Am. Chem. Soc.* **2006**, *128*, 6126–6131.
23. Enyashin, A. N.; Seifert, G. Structure, Stability and Electronic Properties of TiO_2 Nanostructures. *Phys. Status Solidi B* **2005**, *242*, 1361–1370.
24. Fletcher, D. A.; McMeeking, R. F.; Parkin, D. The United Kingdom Chemical Database Service. *J. Chem. Inf. Comput. Sci.* **1996**, *36*, 746–749.